Induction of Type 2 Iodothyronine Deiodinase After Status Epilepticus Modifies Hippocampal Gene Expression in Male Mice

Bruna P. P. Nascimento,[1,2] Barbara M. L. C. Bocco,[3] Gustavo W. Fernandes,[3] Tatiana L. Fonseca,[3] Elizabeth A. McAninch,[3] Carolina V. Cardoso,[4] Eduardo F. Bondan,[4] Renata J. Nassif,[5] Roberta M. Cysneiros,[2] Antonio C. Bianco,[6] and Miriam O. Ribeiro[1,2]

[1]Graduate Program of Translational Medicine, Department of Medicine, Federal University of São Paulo, 04039-002 São Paulo-SP, Brazil; [2]Developmental Disorders Program, Center of Biological Sciences and Health, Mackenzie Presbyterian University, 01302-900 São Paulo-SP, Brazil; [3]Division of Endocrinology and Metabolism, Department of Internal Medicine, Rush University Medical Center, Chicago, Illinois 60612; [4]Department of Environmental and Experimental Pathology, Paulista University, 04026-002 São Paulo-SP, Brazil; [5]Neuroscience Sector, Department of Neurology and Neurosurgery, Federal University of São Paulo, 04039-032 São Paulo-SP, Brazil; and [6]Division of Endocrinology, Department of Medicine, University of Chicago, Chicago, Illinois 60612

Status epilepticus (SE) is an abnormally prolonged seizure that results from either a failure of mechanisms that terminate seizures or from initiating mechanisms that inherently lead to prolonged seizures. Here we report that mice experiencing a 3 hours of SE caused by pilocarpine exhibit a rapid increase in expression of type 2 iodothyronine deiodinase gene (*Dio2*) and a decrease in the expression of type 3 iodothyronine deiodinase gene in hippocampus, amygdala and prefrontal cortex. Type 3 iodothyronine deiodinase in hippocampal sections was seen concentrated in the neuronal nuclei, typical of ischemic injury of the brain. An unbiased analysis of the hippocampal transcriptome of mice undergoing 3 hours of SE revealed a number of genes, including those involved with response to oxidative stress, cellular homeostasis, cell signaling, and mitochondrial structure. In contrast, in mice with targeted disruption of *Dio2* in astrocytes (Astro D2KO mouse), the highly induced genes in the hippocampus were related to inflammation, apoptosis, and cell death. We propose that *Dio2* induction caused by SE accelerates production of T3 in different areas of the central nervous system and modifies the hippocampal gene expression profile, affecting the balance between adaptive and maladaptive mechanisms. (***Endocrinology* 159: 3090–3104, 2018)**

The thyroid gland secretes T4, which is subsequently activated via conversion to T3. T3 binds to nuclear thyroid hormone receptors (TR) and affects the expression of thyroid hormone responsive genes in virtually every tissue and organ including the brain, liver, muscles, adipose tissue, and skeleton (1).

Three different types of iodothyronine deiodinases metabolize T4 and T3 [*i.e.*, type 1, type 2 (D2), and type 3 (D3) iodothyronine deiodinases, each exhibiting different catalytic properties and targeting different iodine residues in the T4 or T3 molecules] (2). D2 catalyzes the outer-ring deiodination of T4, and its expression is widespread in the central nervous system (CNS), primarily in the glial cells; D2-generated T3 enhances thyroid hormone signaling (3–5). Although type 2 iodothyronine deiodinase gene (*Dio2*) is induced by cAMP (6, 7) and mildly suppressed by T3 (8, 9), D2 activity is primarily regulated at a posttranslational level through T4-induced ubiquitination and proteasomal degradation (10, 11).

ISSN Online 1945-7170

Received 8 February 2018. Accepted 6 June 2018.
First Published Online 13 June 2018

Abbreviations: CNS, central nervous system; *Cyclo A*, Cyclophilin A; D2, type 2 iodothyronine deiodinase; D3, type 3 iodothyronine deiodinase; *Dio2*, type 2 iodothyronine deiodinase gene; *Dio3*, type 3 iodothyronine deiodinase gene; FDR, false discovery rate; GSEA, gene set enrichment analysis; PB, phosphate buffer; PF, paraformaldehyde; RT-qPCR, quantitative RT-PCR; SE, status epilepticus; TR, thyroid hormone receptor.

In contrast, D3 is predominantly expressed in neurons, where it terminates thyroid hormone signaling (12, 13) by catalyzing the inner-ring deiodination of T4 and T3 to rT3 and 3,3′-diiodothyronine, respectively. The CNS areas in which it is possible to detect D3 expression in adult rats include the II through IV layers of cerebral cortex, including pyramidal and granulated cells of dentate gyrus, and II layer of piriform cortex (14). Given the reciprocal regulation of *Dio2* and type 3 iodothyronine deiodinase gene (*Dio3*) by thyroid hormone, the presence of these enzymes in the CNS provides a regional adaptation during iodine deficiency (15). In addition, the unique distribution of *Dio2* and *Dio3* expression in different cells of the CNS provides an example of how thyroid hormone signaling is modulated at a local level, relatively independent of circulating levels of T3 (2, 3). In the CNS, D2-generated T3 exits the glial cells and reaches neighboring neurons, where it modulates transcription of T3-responsive genes in a paracrine fashion (16); this mechanism is minimized/modulated by D3 expression in neurons.

Brain ischemia/hypoxia has been shown to acutely induce *Dio3* expression and D3 redistribution to the nucleus, which in cell models reduced the paracrine effects of T3 (17). In contrast, other studies indicate that cerebral ischemia increases D2 activity in cerebral cortex and striatum, whereas the D3 activity remains stable (18). In another study, D2 activity was induced in a cell model by hypoxia without changes in *Dio2* mRNA levels (19). In this case, hypoxia stabilized and prolonged D2's half-life by decreasing its susceptibility to the ubiquitin-proteasome pathway, whereas D3 activity was not affected by hypoxia. Traumatic brain injury was also shown to increase *Dio2* mRNA expression, although it is not clear how much of this effect is due to changes in plasma/local levels of thyroid hormone (8, 20).

Status epilepticus (SE) is an insult to the CNS characterized by a prolonged seizure with loss of consciousness or by sequential seizures of short duration without full recovery of consciousness between them (21, 22). SE may lead to the development of temporal lobe epilepsy that is the most common type of epilepsy among adult subjects and represents ~40% of all epilepsy cases (23, 24). SE causes a myriad of secondary acute seizure-related injuries, including peripheral and brain ischemia and hypoxia (25, 26) that may contribute to neuronal damage and epileptogenesis.

Taking in account that ischemia and hypoxia affect D2 and D3 expression and activities in the CNS, the present investigation tested whether SE modifies thyroid hormone metabolism/action in the brain and how it affects the hippocampal acute transcriptional response.

Material and Methods

Animals

Studies were performed at two sites: Mackenzie Presbyterian University (São Paulo, Brazil) and Rush University Medical Center (Chicago, IL). C57Bl/6J mice were purchased from Center for the Development of Experimental Models for Medicine and Biology, Federal University of São Paulo (São Paulo, Brazil) and from The Jackson Laboratory (Bar Harbor, ME). Astro-D2KO mice were created as described previously (27). Throughout the studies with Astro-D2KO mice, GFAP-Cre animals were used as controls. Only male mice were used, and at the time of the studies all mice were ~8 to 10 weeks old. Animals were maintained at 21 ± 2°C with a continuous 12-hour light: 12-hour dark cycle (lights on at 7:00 AM) and *ad libitum* access to regular chow and water. All drugs and reagents, unless otherwise specified, were purchased from Sigma Chemical Co. (St. Louis, MO). All experiments were carried out in accordance with the Institutional Ethical Committee on Animal Use at Mackenzie Presbyterian University (no. 099/05/2013) and the Institutional Animal Care and Use Committee at Rush University Medical Center (no.15-033) (28).

Induction of SE

SE was induced by pilocarpine or lithium pilocarpine administration.

Pilocarpine-induced SE

Pilocarpine is an alkaloid extracted from Jaborandi (*Pilocarpus jaborandi*) leaves that acts nonselectively on muscarinic acetylcholine receptors inducing SE (29). The anticholinergic scopolamine methyl bromide (Sigma; 1 mg/kg subcutaneously; indicated by Sc in Fig. 1A) was administered to all animals 30 minutes before, to minimize the peripheral cholinergic effects of pilocarpine. Mice were randomly divided in two groups and given pilocarpine hydrochloride (n = 13; 325 mg/kg IP; indicated by P in Fig. 1A) or 0.9% saline (n = 13; indicated by Sa in Fig. 1A). Animals that did not develop SE during the first hour received additional dose of 162.5 mg/kg pilocarpine; if 40 minutes after the second dose the animal still did not develop SE, another injection of 162.5 mg/kg pilocarpine was given, to a maximum of 3 injections. Three hours after the onset of SE, both groups received diazepam (10 mg/kg subcutaneously; indicated by D in Fig. 1A) and, 30 minutes later, animals were anesthetized with urethane (Sigma; 560 mg/kg IP) and euthanized by decapitation or transcardiac perfusion (indicated by K_1 in Fig. 1A). For immunohistochemistry experiments, mice (n = 4) were perfused through the heart and the whole brain removed and fixed. For quantitative RT-PCR (RT-qPCR) experiments, mice (n = 9) brain structures were dissected, immediately frozen in liquid nitrogen, and stored at −80°C until RNA isolation.

Lithium pilocarpine–induced SE

Pilocarpine-induced SE is known for being associated with high mortality (30, 31), which in our hands reached ~65%. Therefore, in some experiments as indicated, mice were given lithium chloride (Sigma; 10 mEq/kg IP; indicated by Li in Fig. 1B) 18 hours before administration of pilocarpine or saline. This lowers the animal's threshold for seizure and a much lower

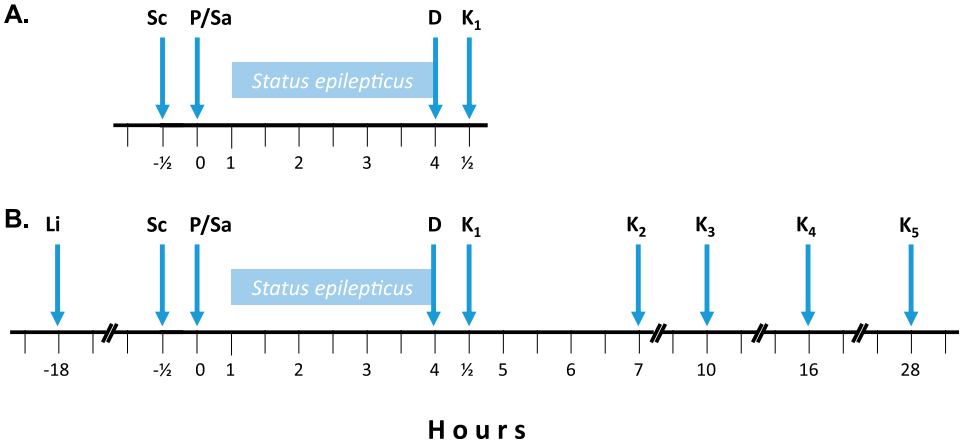

Figure 1. Protocol timeline. (A) Sc was given 30 minutes before P or Sa administration; D was given 3 hours after the onset of SE or an equivalent time in saline injected mice. (B) Same as in panel (A) except that Li was given 18 hours before P or Sa administration; here, animals were also euthanized at longer time points after D administration. D, diazepam; K_1, animals euthanized 30 minutes after D administration; K_2, animals euthanized 3 hours after D administration; K_3, animals euthanized 6 hours after D administration; K_4, animals euthanized 12 hours after D administration; K_5, animals euthanized 24 hours after D administration; Li, lithium chloride; P, pilocarpine; Sa, saline; Sc, methyl scopolamine bromide.

dose of pilocarpine (65 mg/kg IP) can be used, hence reducing mortality to ~25%. Three hours after the onset of SE, both groups received diazepam (10 mg/kg subcutaneously; indicated by D in Fig. 1B) and, 30 minutes later, mice were euthanized by asphyxiation in a carbon dioxide chamber or by transcardiac perfusion after anesthesia with ketamine (100 mg/kg IP) and xylazine (5 mg/kg IP) (indicated by K_1 in Fig. 1B). In some experiments, as indicated, mice were euthanized at different time points after diazepam administration: 3 hours (indicated by K_2 in Fig. 1B), 6 hours (indicated by K_3 in Fig. 1B), 12 hours (indicated by K_4 in Fig. 1B), or 24 hours (indicated by K_5 in Fig. 1B). We also evaluated mice undergoing reduced times of SE, in which case they were euthanized 15 or 30 minutes after the onset of SE.

In all cases, blood samples were collected from the right ventricle after the animals were anesthetized, serum separated, and stored at −80°C.

Perfusion and light microscopy immunohistochemistry for HIF-1α and D3

Mice were anesthetized with urethane (Sigma; 560 mg/kg IP) or with ketamine (100 mg/kg IP) and xylazine (5 mg/kg IP) and underwent transcardiac perfusion at a flow rate of 8 to 10 mL/min first with 0.1M phosphate buffer (PB; pH 7.4) followed by 4% paraformaldehyde (PF; pH 7.4) in 0.1M PB. Brains were removed and immersed in fixative solution of 4% PF for at least 24 hours at room temperature. Later, brains were immersed in 30% sucrose in 0.1M PB for 24 more hours at 4°C. Brains were then kept in 1% PF for at least 24 hours at 4°C. Coronal 50-μM-thick sections through the dorsal hippocampus (Bregma, −1.64) were obtained on a Vibratome (Leica Microsystems, Buffalo Grove, IL) and processed for immunohistochemistry to evaluate the HIF-1α and D3 immunoreactivity. The sections were washed in 0.1M PB three times for 10 minutes each, incubated in BLOXALL™ Endogenous Peroxidase and Alkaline Phosphatase Blocking Solution (Vector Laboratories, Burlingame, CA) for 10 minutes to reduce endogenous peroxidase activity, and rinsed again in 0.1M PB three times for10 minutes each. Then, the sections were incubated in a mixture of 0.5% H_2O_2 and 0.5% Triton X-100 in 0.1M PB for 15 minutes to increase antibody penetration, and rinsed again in 0.1M PB three times for 10 minutes each. The nonspecific antibody binding was blocked by treatment with blocking serum [VECTASTAIN® Elite ABC Kit (rabbit IgG); Vector Laboratories] for 20 minutes followed by incubation in primary antibody. To detect HIF-1α immunoreactivity, the sections were incubated overnight at 4°C in an affinity-purified, rabbit, polyclonal antibody (1:50; catalog no. NB100-479B; RRID: AB_1521173; Novus Biologicals, Littleton, CO); to detect D3 immunoreactivity, the sections were incubated for 36 hours at 4°C in an affinity-purified, rabbit, polyclonal antibody (1:1000; catalog no. NBP1-05767; RRID: AB_1556282; Novus Biologicals). After the incubation with primary antibody, the sections were washed in 0.1M PB three times for 10 minutes each, incubated with biotinylated secondary antibody solution (rabbit IgG; Vector Laboratories) for 2 hours, and then rinsed again in 0.1M PB three times for 10 minutes each. This was followed by incubation with rabbit IgG (Vector Laboratories) for 60 minutes. After this incubation, the sections were washed in 0.1M PB three times for 10 minutes each, and the complex antigen-antibody was visualized using diaminobenzidine (DAB Peroxidase Substrate; Vector Laboratories). Finally, the sections were rinsed again in 0.1M PB and mounted onto glass slides, dried, dehydrated in ethanol from 80% to 100%, diaphanized in xylol, and coverslipped with Entellan (Merck, Kenilworth, NJ). Quantification of HIF-1α signal was performed in 20 slides of each group using Image Pro Plus 6.0 software (Media Cybernetics, Inc., Bethesda, MD) calibrated with digital color filters so that only immunostained areas were identified automatically and background staining excluded from the measurement. Results were expressed per area analyzed relative to the total area, with 0 being absence of staining and 1 staining of the entire area.

mRNA analysis by RT-qPCR

Total tissue RNA was extracted using either the RNeasy® Plus Universal Mini Kit (Qiagen, Germantown, MD) or RNeasy® Lipid Tissue Mini Kit (Qiagen) and digested with DNase using the RNase-Free DNase Set (Qiagen). RNA was quantified using the NanoDrop 2000 spectrophotometer

(Thermo Fisher, Waltham, MA), and 1.0 μg of total RNA was used to synthesize cDNA using either the SuperScript® III First-Strand Synthesis SuperMix for qRT-PCR (Invitrogen, Carlsbad, CA) in a Mastercycler® Gradient thermocycler (Eppendorf, Hauppauge, NY) or the Transcriptor First Strand cDNA Synthesis Kit (Roche) in a Mastercycler® pro thermocycler (Eppendorf). Genes of interest were analyzed (Eco™ Real-Time PCR System; Illumina/Step-one real-time PCR system; Step-one-plus real-time PCR system; Applied Biosystems, Foster City, CA) using either QuantiTect™ SYBR® Green (Qiagen) or PerfeCTa SYBR Green Fastmix Rox (Quantas, Beverly, MA). Standard curves were built with 3 to 4 points of serially diluted (factor of 5) mixed experimental and control group cDNA; $r > 0.95$ for all curves of hippocampus, >0.98 for all curves of amygdala, and >0.97 for all curves of prefrontal cortex; amplification efficiency of 50% to 100% for the hippocampus, 42% to 93% for the amygdala, and 69% to 102% for the prefrontal cortex. Relative expression of genes of interest was expressed as a function of the housekeeping internal control gene Cyclophilin A (*Cyclo A*). The PCR program consisted in 2 minutes at 50°C, a hot start of 95°C for 15 minutes, 40 to 50 cycles of 15 seconds at 94°C, 30 seconds at 60°C, 30 seconds at 72°C, followed by a melt curve of 15 seconds at 95°C, 15 seconds at 55°C and 15 seconds at 95°C. All primer sequences used in this study are listed in Supplemental Table 1. Mir128-1 mRNA analysis was performed using Taqman reagents (assay IDMm04238113_s1; catalog no. 4426961; Applied Biosystems) with the following conditions: 95°C for 20 seconds, followed by 40 cycles of 1 second at 95°C and 20 seconds at 60°C. *Cyclo A* was also used as an internal control gene, and there was no difference in its expression between the groups.

Microarray analysis

Total tissue RNA was extracted from hippocampus of Astro-D2KO mice and their control using the RNeasy® Lipid Tissue Mini Kit (Qiagen). The DNase treatment was performed using the RNase-Free DNase Set (Qiagen). RNA was quantified using a NanoDrop spectrophotometer, and RNA quality and integrity were analyzed by electrophoresis in a 1% denaturing agarose gel stained with ethidium bromide. Microarray analysis was performed by the Joslin Diabetes Center Genomics Core Laboratory (Boston, MA). Gene expression was evaluated using Affymetrix GeneChip® Mouse Gene 2.0 ST arrays (Affymetrix, Santa Clara, CA); gene expression data was preprocessed using Affymetrix Expression Console software. Differential expression analysis was performed with Affymetrix Transcriptome Analysis Console. One-way ANOVA was used to calculate *P* values for each fold change (linear); multitesting correction was then performed using the Benjamini-Hochberg Step-Up false discovery rate (FDR)–controlling procedure for all the expressed genes. The differentially expressed genes were considered statistically significant with an ANOVA $P < 0.05$; gene set enrichment analysis (GSEA) used the Broad Institute platform. Expression values for all genes from all hippocampus samples were used in the analysis; no filter was applied to eliminate genes with low expression. GSEA included calculation of enrichment scores, estimation of significance level of enrichment scores (nominal *P* value), and adjustment for multiple hypothesis testing including the normalized enrichment score and FDR. A nominal *P* value <1% was chosen to indicate significance.

Deiodinase activity and serum T3 and T4 levels

Deiodinase activities were assayed in tissue sonicates as previously described (32).

Serum T3 and T4 were measured using an enzyme-linked immunosorbent assay kit from CUSABIO (CSB-E05086m and CSB-E05083m; Atlanta, GA) using an in-house standard curve prepared with mouse charcoal-stripped serum (28). In sum, 35 μL of standard or samples were added in a 96-well plate. Then, 50 μL of conjugate reagent was subsequently added and the plate was incubated for 60 minutes at 37°C. Wells were aspirated and washed three times using 200 μL of wash buffer. Next, 50 μL of horseradish peroxidase–avidin reagent was added, and the plate incubated for 30 minutes at 37°C. Wells were aspirated and washed three times using 200 μL of wash buffer. Then, 50 μL of substrate A and B were added and the plate was incubated for 15 minutes at 37°C in the dark. Stop solution was added and the optical density measured within 10 minutes using a microplate reader set to 450 nm. Data were plotted and calculated using a four-parameter logistic curve fit.

Statistical analyses

All data were analyzed using PRISM software (GraphPad Software) and are expressed as mean ± SEM. Comparisons between two groups were analyzed with a two-tailed Student *t* test; comparisons between more than two groups were analyzed by one-way ANOVA followed by the Newman-Keuls multiple comparison test to detect differences between groups. $P < 0.05$ was considered statistically significant.

Results

SE in mice

SE in mice initiated 30 to 40 minutes after pilocarpine administration (indicated by P in Fig. 1) and was interrupted 3 hours later with diazepam (indicated by D in Fig. 1). About 13% of the animals receiving pilocarpine did not exhibit SE and were considered later as indicated. Many genes are known to be affected by SE. For example, mRNA levels of *Bdnf*, *Ngf*, and *Egr1* were elevated in the hippocampus, prefrontal cortex, and amygdala (Fig. 2A–2I), whereas *Ntf3* was universally downregulated (Fig. 2J–2L) after 3 hours of SE in animals euthanized 30 minutes later. Seizure was stopped by diazepam (indicated by K_1 in Fig. 1A). To evaluate whether the 3 hours of SE resulted in hypoxia, HIF-1α immunostaining was assessed in the hippocampal formation and showed an increase in all hippocampus, especially in the CA1 region (Fig. 2M–2R).

Deiodinase activity and serum T3 and T4 levels

Dio3 mRNA levels were reduced in the hippocampus, prefrontal cortex, and amygdala (Fig. 3A–3C), whereas D3 activity remained stable, mildly reduced in the amygdala (Fig. 3G–3I). However, D3 immunostaining was enhanced, given its transit to the neuronal nuclei (Fig. 3M–3V). *Dio2* expression increased in the three regions (Fig. 3D–3F) and there was activity only in the

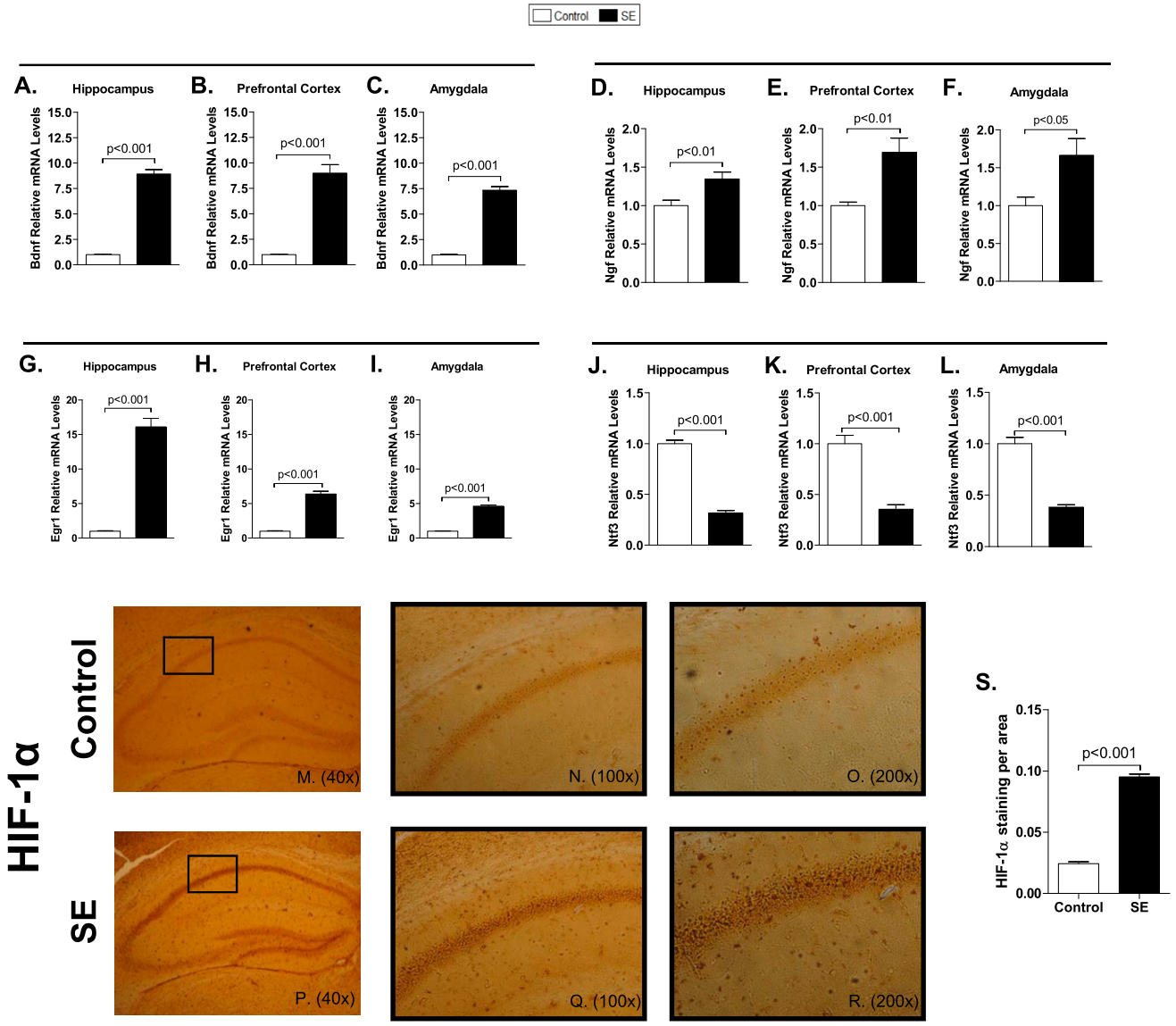

Figure 2. mRNA levels of typical genes affected by seizures and HIF-1α staining in C57Bl/6J mice following 3 hours of SE. In all cases, SE was induced by pilocarpine administration, as in Fig. 1A. *Bdnf* mRNA levels in (A) hippocampus, (B) prefrontal cortex, and (C) amygdala measured by RT-qPCR and using *Cyclo A* as internal control (n = 9). *Ngf* mRNA levels in (D) hippocampus, (E) prefrontal cortex, and (F) amygdala measured by RT-qPCR and using *Cyclo A* as internal control (n = 9). *Egr1* mRNA levels in (G) hippocampus, (H) prefrontal cortex, and (I) amygdala measured by RT-qPCR and using *Cyclo A* as internal control (n = 9). *Ntf3* mRNA levels in (J) hippocampus, (K) prefrontal cortex, and (L) amygdala measured by RT-qPCR and using *Cyclo A* as internal control (n = 9). Values represent the mean ± SEM. (M–R) Low-power magnification images showing immunohistochemical analysis of HIF-1α in hippocampus (n = 4); (N, Q) ×100 and (O, R) ×200 magnifications of the CA1 field. (S) HIF-1α signal expressed per area in hippocampal CA1 field; values are mean ± SEM.

hippocampus and cerebral cortex (Fig. 3J–3L). Changes in *Dio2* and *Bdnf* expression in the hippocampus occurred rapidly, after only 15 or 30 minutes of seizure initiation (Fig. 4A and 4B). *Dio2* mRNA levels and activity returned to baseline shortly after diazepam was injected (Fig. 4C–4D). Notably, at later time points, D2 activity decreased markedly, to <50% of baseline levels (Fig. 4D). In contrast, *Dio3* expression remained low throughout the observation period, but D3 activity never decreased (Fig. 4E–4F). Notably, neither *Dio2* nor *Bdnf* mRNA levels was modified in a subset of mice that are refractory to pilocarpine-induced seizure (Fig. 4G–4H). This indicates that changes in *Dio2* expression following SE are due to increased neuronal activity caused by seizures and not to pilocarpine or diazepam *per se*. Circulating T3 [control (n = 4): 0.35 ± 0.04 vs SE (n = 5): 0.36 ± 0.01 ng/mL] and T4 levels [control (n = 4): 64.53 ± 14.3 vs SE (n = 5): 73.55 ± 8.48 ng/mL] remained unaffected by 3 hours of SE.

Unbiased hippocampal gene expression in mice experiencing 3 hours of SE

To understand the role played by D2 in the modifications of CNS gene expression associated with SE, we

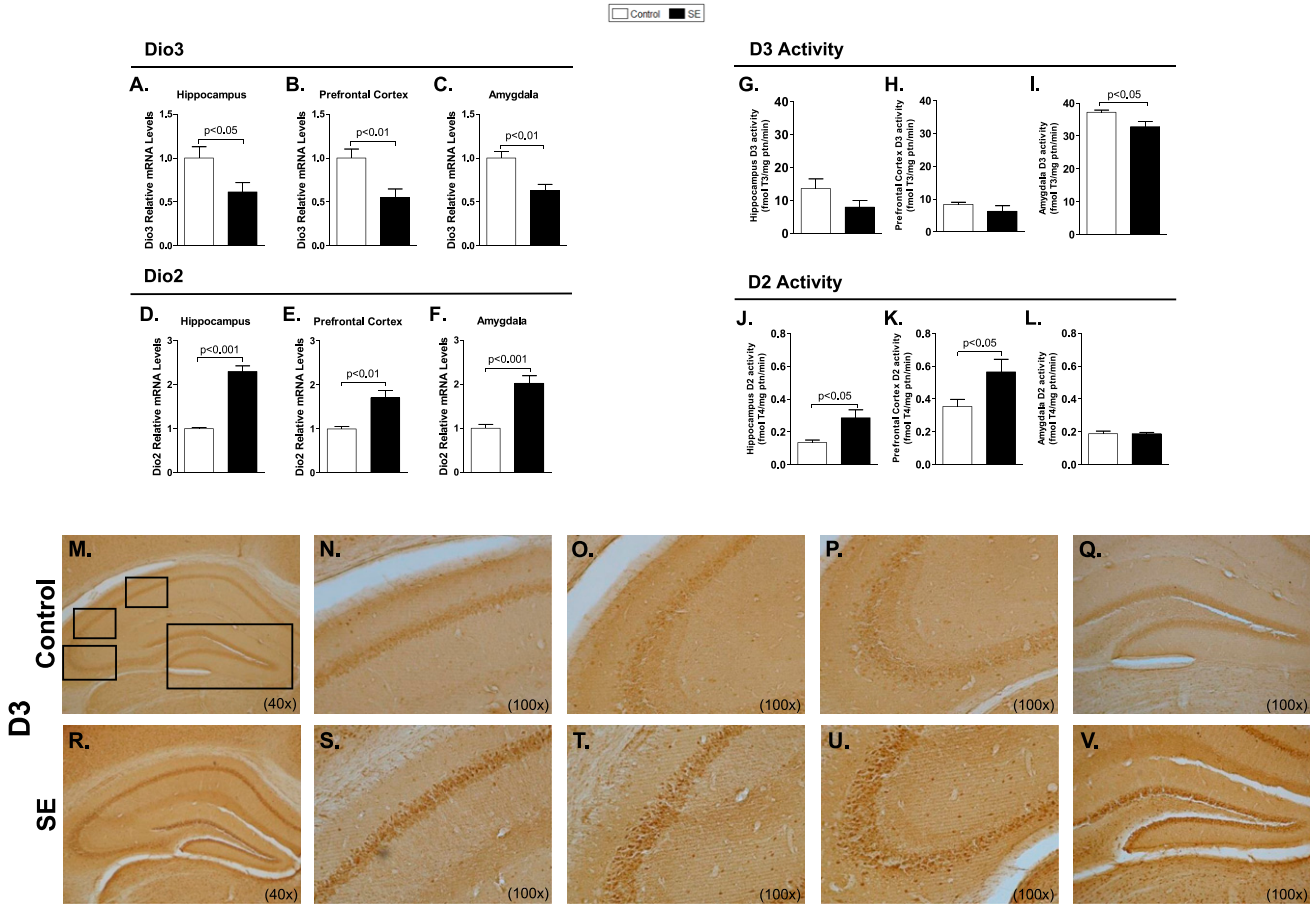

Figure 3. Deiodinase expression and activity and D3 staining in C57Bl/6J mice following 3 hours of SE. *Dio3* mRNA levels in (A) hippocampus, (B) prefrontal cortex, and (C) amygdala measured by RT-qPCR and using *Cyclo A* as internal control (n = 9). *Dio2* mRNA levels in (D) hippocampus, (E) prefrontal cortex, and (F) amygdala measured by RT-qPCR and using *Cyclo A* as internal control (n = 9). (G–L) SE was induced by lithium chloride and pilocarpine administration, as in Fig. 1B; animals were euthanized at K_1. D3 activity in (G) hippocampus, (H) prefrontal cortex, and (I) amygdala (n = 5). D2 activity in (J) hippocampus, (K) prefrontal cortex, and (L) amygdala (n = 5). Values represent mean ± SEM. (M–V) SE was induced by pilocarpine administration, as in Fig. 1A. Low-power magnification images showing immunohistochemical analysis of D3 in hippocampus (n = 4): (M, R) ×40 magnification of hippocampus, (N–Q, S–V) high magnifications of the black boxes in (M) and (R), respectively: (N, S) ×100 magnification of CA1 field, (O, T) ×100 magnification of CA2 field, (P, U) ×100 magnification of CA3 field, and (Q, V) ×100 magnification of the dentate gyrus.

focused on the hippocampus and performed an unbiased gene expression analysis using microarray of hippocampal RNA obtained 3 hours after seizure was stopped (indicated by K_2 in Fig. 1B); a time chosen based on the time-course data (Fig. 5D–5F). For these experiments, we also used Astro-D2KO mice (and their CRE-GFAP controls), in which *Dio2* is selectively inactivated in glial cells (27). Here also, circulating T3 [Astro-D2KO (n = 5): 0.34 ± 0.02 vs Astro-D2KO-SE (n = 4): 0.38 ± 0.01 ng/mL] and T4 levels [Astro-D2KO (n = 5): 60.39 ±1 2.47 vs Astro-D2KO-SE (n = 4): 76.98 ± 11.86 ng/mL] remained unaffected by 3 hours of SE.

The differential expression analysis of control vs control-SE hippocampus RNA indicated that in control-SE mice, 3934 transcripts were modified at a P value < 0.01, of which 1602 were up- and 2332 downregulated. If a threefold cutoff was used, these numbers were reduced to 128 and 3 (Supplemental Table 2), respectively, with the top 20 upregulated genes being involved in neuronal plasticity, response to stress, and inflammation (Table 1). The same analysis was done for Astro-D2KO vs Astro-D2KO-SE hippocampus RNA. In these animals, SE modified the expression of 4402 transcripts, of which 1696 were up- and 2706 downregulated. With the threefold cutoff, these numbers were reduced to 104 and 3 (Supplemental Table 3), respectively. The list of top five genes in both animals is very similar, but with markedly reduced fold induction in Astro-D2KO-SE animals (Table 1). It is also noticeable that genes that ranked high in the control-SE are in general ranked low in the Astro-D2KO-SE and vice versa (Table 1).

Although several common genes were affected by SE in both control and Astro-D2KO animals (2416 transcripts; Supplemental Table 4 for > 3-fold change), we noticed that a substantial number of genes (1518 transcripts) were only affected by SE in control animals, 6 of

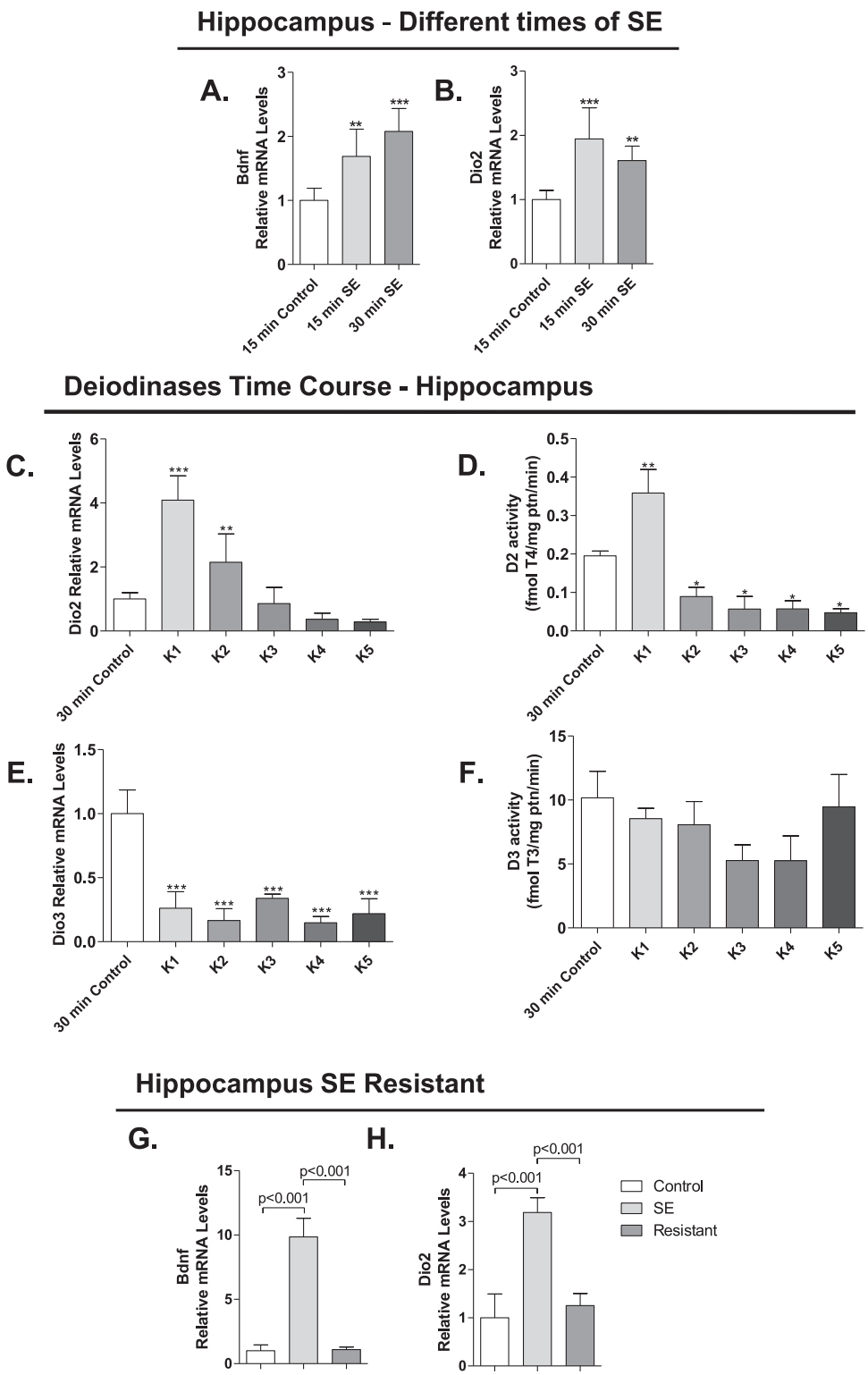

Figure 4. Gene expression and deiodinases activity in mice after 3 hours of SE. In all cases, SE was induced by lithium chloride and pilocarpine administration, as in Fig. 1B. (A) *Bdnf* mRNA levels in hippocampus of C57Bl/6J mice undergoing different times of SE (15 and 30 minutes); measurements by RT-qPCR using *Cyclo A* as internal control; given the short duration of the SE, animals were not treated with diazepam (saline, n = 6; 15 minutes, n = 7; 30 minutes, n = 4). (B) *Dio2* mRNA levels in hippocampus of C57Bl/6J mice undergoing different times of SE (15 and 30 minutes) measured by RT-qPCR and using *Cyclo A* as internal control; as before, SE animals were not treated with diazepam (saline, n = 7; 15 and 30 minutes, n = 5). (C) *Dio2* mRNA levels in hippocampus of C57Bl/6J mice euthanized in different times (K_1, K_2, K_3, K_4, and K_5) after diazepam injection measured by RT-qPCR and using *Cyclo A* as internal control (control, n = 5; K_1, n = 5; K_2, n = 4; K_3, n = 3; K_4, n = 4; K_5, n = 4). (D) D2 activity in hippocampus of C57Bl/6J mice euthanized in different times (K_1, K_2, K_3, K_4, and K_5) after diazepam injection (control, n = 4; K_1, n = 4; K_2, n = 4; K_3, n = 3; K_4, n = 4; K_5, n = 4). (E) *Dio3* mRNA levels in hippocampus of C57Bl/6J mice euthanized at different times (K_1, K_2, K_3, K_4, and K_5) after diazepam injection measured by RT-qPCR and using *Cyclo A* as internal control (control, n = 4; K_1, n = 5; K_2,

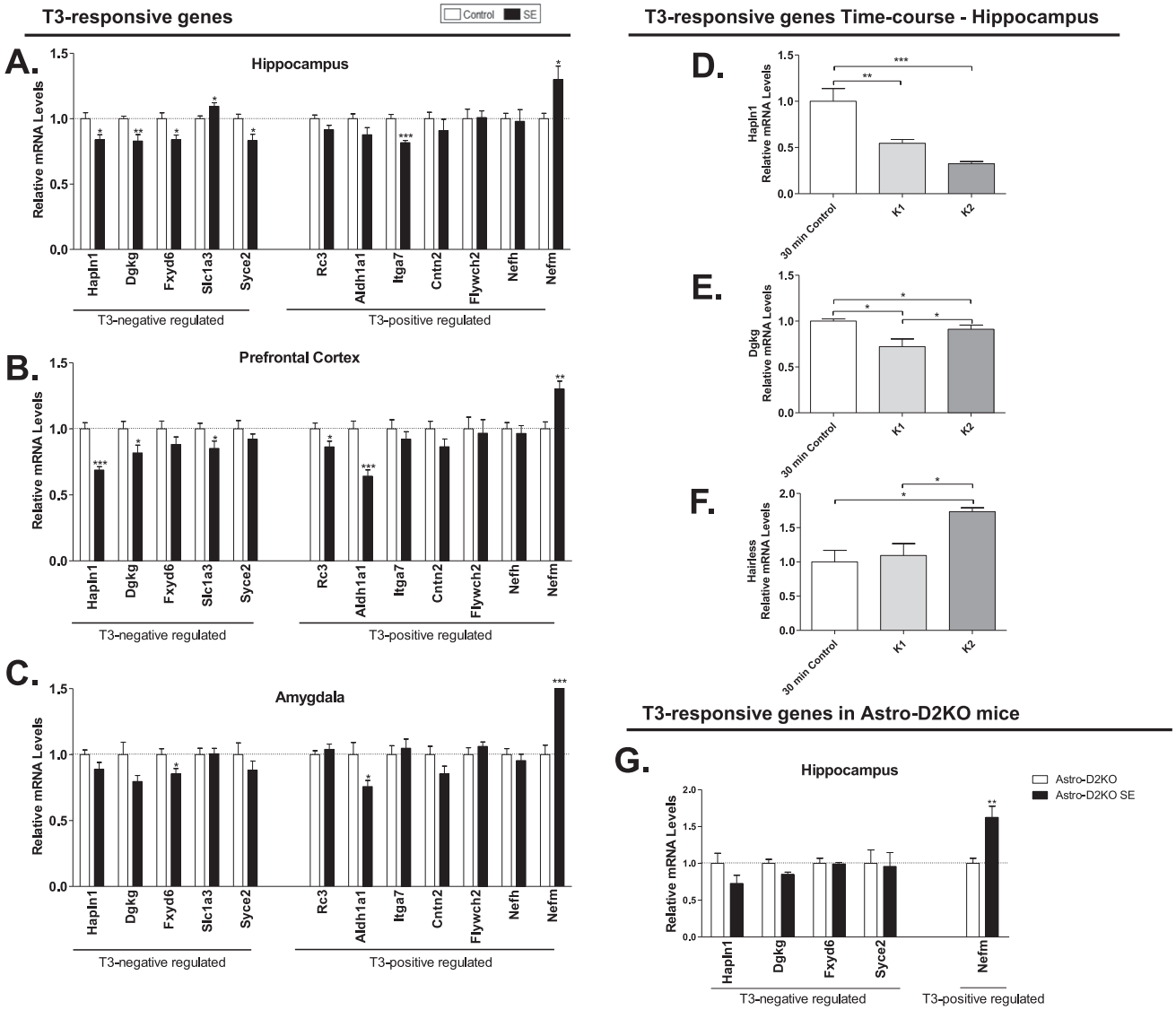

Figure 5. mRNA levels of T3-responsive genes in mice after SE. (A–C) SE was induced by pilocarpine administration, as in Fig. 1A. (D–G) SE was induced by lithium chloride and pilocarpine administration, as in Fig. 1B. T3-responsive gene mRNA levels in (A) hippocampus, (B) prefrontal cortex, and (C) amygdala of C57Bl/6J mice following pilocarpine-induced SE that were euthanized 30 minutes after diazepam injection, measured by RT-qPCR and using *Cyclo A* as internal control (n = 9). (D–F) T3-responsive gene mRNA levels in hippocampus of C57Bl/6J mice following lithium pilocarpine–induced SE that were euthanized 30 minutes and 3 hours after diazepam injection, measured by RT-qPCR and using *Cyclo A* as internal control (control, n = 5; K_1, n = 5; K_2, n = 4). (D) *Hapln1*, (E) *Dgkg*, (F) hairless, and (G) T3-responsive gene mRNA levels in hippocampus of Astro-D2KO mice following lithium pilocarpine–induced SE that were euthanized 3 hours after diazepam injection, measured by RT-qPCR and using *Cyclo A* as internal control. Values represent mean ± SEM *$P < 0.05$ vs control; **$P < 0.01$ vs control; ***$P < 0.001$ vs control.

which previously identified as being responsive to T3 in cerebral cortex and/or striatum (*i.e.*, *Luzp1*, *Paqr6*, *Shh*, *Cirbp*, *Hapln1*, and *Nrgn*) (33–35). Considering fold change > 2, this number dropped to 36 genes (Table 2). Using the same criteria, the 1986 transcripts that were affected by SE only in Astro-D2KO dropped to 28 genes (Table 3). A major difference between these lists is the presence of several mitochondrial-related genes in control-SE and several inflammation-related genes in the Astro-D2KO–SE samples (Tables 2 and 3).

We also compared the complete set of genes modified by SE in control vs Astro-D2KO mice using GSEA at a nominal P value < 1% (Supplemental Table 5). GSEA revealed that 88 gene sets were enriched and 8

Figure 4. (Continued). n = 4; K_3, n = 2; K_4, n = 4; K_5, n = 4). (F) D3 activity in hippocampus of C57Bl/6J mice euthanized in different times (K_1, K_2, K_3, K_4, and K_5) after diazepam injection (control, n = 4; K_1, n = 2; K_2, n = 4; K_3, n = 3; K_4, n = 4; K_5, n = 4). (G) *Bdnf* mRNA levels in hippocampus of GFAP-Cre animals resistant to pilocarpine measured by RT-qPCR and using *Cyclo A* as internal control (control, n = 4; SE, n = 4; resistant, n = 4). (H) *Dio2* mRNA levels in hippocampus of GFAP-Cre animals resistant to pilocarpine measured by RT-qPCR and using *Cyclo A* as internal control (control, n = 4; SE, n = 3; resistant, n = 3). Values represent the mean ± SEM *$P < 0.05$ vs control; **$P < 0.01$ vs control; ***$P < 0.001$ vs control.

Table 1. Hippocampal Genes Enriched in Both Control-SE and Astro-D2KO-SE

		Control-SE		Astro-D2KO-SE	
Gene Symbol	**Description**	**Rank**	**Fold**	**Rank**	**Fold**
Npas4	Neuronal PAS domain protein 4	1	46	3	23
Hspa1b	Heat shock protein 1B	2	37	1	28
Hspa1a	Heat shock protein 1A	3	36	2	26
Fosb	FBJ osteosarcoma oncogene B	4	27	5	18
Fos	FBJ osteosarcoma oncogene	5	18	6	14
Inhba	Inhibin β-A	6	17	13	9
Ccl3	Chemokine (C-C motif) ligand 3	7	16	4	22
Egr1	Early growth response 1	8	11	15	9
Atf3	Activating transcription factor 3	9	11	18	8
Tnfrsf23	Tumor necrosis factor receptor superfamily, member 23	10	11	21	7
Egr4	Early growth response 4	11	10	19	7
Pcsk1	Proprotein convertase subtilisin/kexin type 1	12	10	10	11
Arc	Activity regulated cytoskeletal-associated protein	13	9.4	24	6
Nr4a1	Nuclear receptor subfamily 4, group A, member 1	14	9.2	14	9.2
Lilrb4	Leukocyte immunoglobulin-like receptor, subfamily B, member 4	15	8.8	9	13
Nr4a2	Nuclear receptor subfamily 4, group A, member 2	19	7.6	7	13
Serpinb2	Serine (or cysteine) peptidase inhibitor, clade B, member 2	—	—	8	13
Nts	Neurotensin	27	6.1	11	10
Gadd45g	Growth arrest and DNA-damage-inducible 45 γ	20	7.0	12	10

Differential expression was at $P < 0.01$ and a fold change ≥ 3 or ≤ -3 in control-SE (n = 4) and Astro-D2KO-SE (n = 4) hippocampus.

impoverished in control-SE, whereas in the Astro-D2KO-SE 96 gene sets were enriched and 5 impoverished. There are 28 enriched gene sets common to control and Astro-D2KO animals, representing those genes that are modified by SE independently of D2 expression (Supplemental Table 4). In contrast, of the 141 gene sets that were affected by D2 expression or lack thereof, 68 were enriched in the control animals only and 73 in the Astro-D2KO animals only (Supplemental Table 5). The top 10 gene sets enriched in control-SE include genes involved in response to oxidative stress, cell signaling, and homeostasis (Table 4). In contrast, the top gene sets enriched in Astro-D2KO-SE include transfer of phosphorus-containing groups and kinase activity (Table 4). These findings were confirmed by RT-qPCR of representative genes from each of these gene sets (Fig. 6A–6H).

Expression of typical T3-responsive genes in the CNS of mice following SE

We used RT-qPCR to test whether induction of D2 activity by SE was associated with changes in the expression of typical T3-responsive genes. We looked at two sets of genes: five negatively and seven positively regulated by T3 in the CNS (35). In the hippocampus, SE reduced the expression of four genes negatively regulated by T3 (*i.e.*, *Hapln1*, *Dgkg*, *Fxyd6*, and *Syce2*), whereas it increased the expression of one gene positively regulated by T3 (*i.e.*, *Nefm*) (Fig. 5A). Two genes responded with the opposite behavior, *Slc1a3* and *Itga7*, whereas other T3-responsive genes were not affected (Fig. 5A). A similar general pattern was observed in the prefrontal cortex (Fig. 5B) and amygdala (Fig. 5C), albeit the latter was only minimally responsive to T3. A time-course analysis of three representative genes in the hippocampus indicated a progressive decrease in *Hapln1* mRNA and a time-dependent increase in hairless mRNA, whereas *Dgkg* mRNA levels went down by 30 minutes and recovered almost fully by 3 hours (Fig. 5D–5F). That the response to T3 was predominantly on the negatively regulated genes is reminiscent of the fact that negatively regulated genes by T3 tend to be more dependent of D2-generated T3 than on plasma T3 (34). Dependency on *Dio2* activation was confirmed by studying those 5 T3-regulated genes in Astro-D2KO mice after 3 hours of SE (Fig. 5G). The four negatively regulated genes (*i.e.*, *Hapln1*, *Dgkg*, *Fxyd6*, and *Syce2*) were no longer affected by 3 hours of SE, whereas the positively regulated gene (*i.e.*, *Nefm*) remained responsive to 3 hours of SE (Fig. 5G).

Discussion

The current study revealed that SE in mice rapidly increases CNS *Dio2* expression, which greatly modifies hippocampal gene expression profile and its response to SE (Tables 1–4). Within 30 minutes of SE interruption (indicated by K_1 in Fig. 1A), there is doubling of *Dio2* expression in the hippocampus, prefrontal cortex, and amygdala (Fig. 3D–3F) that is accompanied by a decrease

Table 2. Individual Transcripts Affected by SE in Hippocampus of Control-SE Mice

Gene Symbol	Description	Fold Change	*P*
	Genes Modified in Control-SE Hippocampus Only		
Angiogenesis			
n-R5s87	Nuclear encoded rRNA 5S 87	3.46	0.003093
Mir128-2	microRNA 128-2	2.19	0.001731
Cell cycle and proliferation			
Cks2	CDC28 protein kinase regulatory subunit 2; cyclin-dependent kinases regulatory subunit 2-like; predicted gene 12891; predicted gene 15452	2.73	0.002548
Mnd1	Meiotic nuclear divisions 1 homolog (*Saccharomyces cerevisiae*)	2.62	0.002064
Mir136	microRNA 136; mmu-mir-136; mmu-mir-3071	2.2	0.006001
Lcmt2	Leucine carboxyl methyltransferase 2	2.19	0.004942
Cdk6	Cyclin-dependent kinase 6	2.15	0.008803
Mir708	microRNA 708	2.13	0.000156
Cell death mechanisms			
Mir376a	microRNA 376a	2.32	0.009128
Enzymes			
Acat3	Acetyl-coenzyme A acetyltransferase 3	2.59	0.002661
Nanp	N-acetylneuraminic acid phosphatase	−2.17	0.001961
Mitochondrial function			
mt-Tk	Mitochondrially encoded tRNA lysine	6.39	0.002554
mt-Tt	Mitochondrially encoded tRNA threonine	4.81	0.001726
mt-Tt	Mitochondrially encoded tRNA threonine	4.64	0.002216
mt-Ts2	Mitochondrially encoded tRNA serine 2; mitochondrially encoded tRNA leucine 2	3.85	0.003586
mt-Ts2	Mitochondrially encoded tRNA serine 2	3.29	0.007613
mt-Ty	Mitochondrially encoded tRNA tyrosine	2.1	0.00825
Histones			
Hist2h3b	Histone cluster 2, H3b; histone cluster 1, H3e; histone cluster 1, H3b; histone cluster 1, H3d; histone cluster 1, H3c; histone cluster 1, H3f; histone cluster 2, H3c2; histone cluster 2, H3c1	3.32	0.004662
Hist1h3d	Histone cluster 1, H3d	2.03	0.000865
Inflammation			
Stk40	Serine/threonine kinase 40	2.77	0.00856
Extracellular matrix			
Gm13034	SWI/SNF related, matrix associated, actin dependent regulator of chromatin, subfamily a, member 5 pseudogene	2.53	0.000736
Tinag	Tubulointerstitial nephritis antigen	2.34	0.006487
Dsp	Desmoplakin	−3.49	0.002388
Glt8d2	Glycosyltransferase 8 domain containing 2	−2.09	0.000497
Neural plasticity			
Emp1	Epithelial membrane protein 1	3.25	0.00215
Neuroprotective mechanisms			
Dnajb5	DnaJ (Hsp40) homolog, subfamily B, member 5	2.12	0.00161
Snord14e	Small nucleolar RNA, C/D box 14E; heat shock protein 8	2.01	0.001037
Neurotransmitter signaling			
Sstr2	Somatostatin receptor 2	2.31	0.007373
Gucy2c	Guanylate cyclase 2c	2.16	0.002788
Dok5	Docking protein 5	2.08	0.004218
Per2	Period circadian clock 2	2.04	0.002296
Ttc26	Tetratricopeptide repeat domain 26	−2.12	0.006375
Ttc26	Tetratricopeptide repeat domain 26	−2.12	0.006375
Slc22a8	Solute carrier family 22 (organic anion transporter), member 8	−2.45	0.007346
Transcription factors			
Hes5	Hairy and enhancer of split 5 (Drosophila)	−2	0.001097

Differential expression was at a $P < 0.01$ and a fold change ≥2 or ≤−2 in control-SE (n = 4) hippocampus.

in *Dio3* mRNA levels (Fig. 3A–3C), albeit D3 activity was not modified within the observation time frame (Fig. 3G–3I). Whereas several T3-responsive genes in the CNS were affected as a result of the SE-induced *Dio2* expression (Fig. 5), an unbiased analysis of the hippocampal transcriptome using mice with targeted disruption of *Dio2* in astrocytes revealed a much broader effect of *Dio2* presence (Tables 1–4). In fact, several genes and gene sets were modified by SE in mice with a functional D2 pathway only, which were mostly related

Table 3. Individual Transcripts Affected by SE in Hippocampus of Astro-D2KO-SE Mice

Gene Symbol	Description	Fold Change	*P*
	Genes Modified in Astro-D2KO-SE Hippocampus Only		
Apoptosis			
Mir128-1	microRNA 128-1	2.17	0.00109
Enzymes			
Arxes1	Adipocyte-related X-chromosome expressed sequence 1; adipocyte-related X-chromosome expressed sequence 2	2.05	0.000814
B3gnt5	UDP-GlcNAc: β Gal β-1,3-*N*-acetylglucosaminyltransferase 5	2.03	0.000779
Pi15	Peptidase inhibitor 15	2	0.001314
Nt5c1a	5-nucleotidase, cytosolic IA	2	0.001601
Aspa	Aspartoacylase	−2.03	0.004198
Extracellular matrix			
Grem2	gremlin 2 homolog, cysteine knot superfamily (*Xenopus laevis*)	2.67	0.000002
Hs3st5	heparan sulfate (glucosamine) 3-*O*-sulfotransferase 5	2.08	0.00285
Inflammation			
Serpinb2	Serine (or cysteine) peptidase inhibitor, clade B, member 2	13.01	0.000372
Ctla2a	Cytotoxic T lymphocyte-associated protein 2 α	2.6	0.00251
Msr1	Macrophage scavenger receptor 1	2.04	0.003938
Il11	Interleukin 11	2.02	0.007672
Sbno2	Strawberry notch homolog 2 (*Drosophila*)	2.4	0.007635
Membrane transporters			
Slc10a6	Solute carrier family 10 (sodium/bile acid cotransporter family), member 6	2.18	0.007324
Neural plasticity			
Zfp804a	Zinc finger protein 804A	2.46	0.002032
Gdnf	Glial cell line derived neurotrophic factor	2.03	0.001031
Mir344e	microRNA 344e	−2.36	0.000517
Ptch1	Patched homolog 1	−2.13	0.000437
Neurotransmitter signaling			
Penk	Preproenkephalin; short chain dehydrogenase/reductase family 39U, member 1	2.47	0.004063
Gfra1	Glial cell line derived neurotrophic factor family receptor α 1	2.43	0.002592
Smim3	Small integral membrane protein 3	2.22	0.00379
Other			
Ccdc138	Coiled-coil domain containing 138	2.22	0.008305
Snord107	Small nucleolar RNA, C/D box 107; SNRPN upstream reading frame	−2.38	0.001387
Mir1839	microRNA 1839; RIKEN cDNA 2900076A07 gene	−2.18	0.005299
Oxidative stress			
Gpx8	Glutathione peroxidase 8 (putative)	2.19	0.001493
Transcription factor			
Osr1	Odd-skipped related 1 (*Drosophila*)	−2.01	0.001485

Differential expression was at $P < 0.01$ and a fold change ≥ 2 or ≤ -2 in Astro-D2KO-SE (n = 4) hippocampus.

to mitochondrial function and oxidative stress (Tables 1 and 2). In contrast, the profile of SE-induced genes in the animals with inactive *Dio2* included peptidase inhibitors, cytokines, and genes involved in inflammation and apoptosis (Tables 1 and 3). This is reminiscent of recent findings that bleomycin-induced lung injury in mice causes *Dio2* activation and local T3 production that promotes mitochondrial biogenesis, improved mitochondrial bioenergetics, and weakened mitochondria-regulated apoptosis in alveolar epithelial cells (36). It is notable that the relatively low overlap of the genes potentially regulated by *Dio2* in this model and those reportedly regulated by T3 in other datasets. This may be due to differences in brain region, developmental stages, or the possibility that genes primarily affected by *Dio2* are few compared with those affected by SE via other mechanisms.

Although pilocarpine binds to all muscarinic acetylcholine receptor subtypes (29), only the M1 receptor mediates seizures via its typical downstream signaling pathway, DAG and IP3. M1Rs are expressed both in neurons and astrocytes, mostly in the cerebral cortex and hippocampus. However, once seizure activity settles in, there is increased expression of cAMP-responsive genes that occurs most likely as a result of increased glutamate release (37–40). Notably, *Dio2* is highly responsive to cAMP (6), hence the likely mechanism through which *Dio2* expression is increased in the current study. CNS accumulation of cAMP requires and is secondary to

Table 4. GSEA of Genes Affected by SE in Control vs Astro-D2KO Mice

Gene Ontology	Description	Total No. Genes in Set	ES	NES	Nominal *P*	FDR q Value
Enriched in control-SE animals						
GO:0006979	Response to oxidative stress	40	−0.39	−1.35	0	0.276
GO:0019932	Second-messenger–mediated signaling	140	−0.47	−1.34	0	0.276
GO:0007267	Cell–cell signaling	369	−0.42	−1.35	0	0.277
GO:0045597	Positive regulation of cell differentiation	24	−0.68	−1.36	0	0.279
GO:0009991	Response to extracellular stimulus	33	−0.65	−1.37	0	0.281
GO:0019725	Cellular homeostasis	133	−0.48	−1.37	0	0.281
GO:0009887	Organ morphogenesis	139	−0.43	−1.37	0	0.282
GO:0048878	Chemical homeostasis	139	−0.48	−1.37	0	0.284
GO:0008284	Positive regulation of cell proliferation	128	−0.49	−1.38	0	0.291
GO:0030234	Enzyme regulator activity	294	−0.36	−1.38	0	0.292
Enriched in AstroD2KO-SE animals						
GO:0016772	Transferase activity transferring phosphorus-containing groups	392	−0.26	−1.26	0	0.366
GO:0004672	Protein kinase activity	261	−0.31	−1.3	0	0.371
GO:0051239	Regulation of multicellular organismal process	139	−0.45	−1.29	0	0.373
GO:0016301	Kinase activity	340	−0.27	−1.29	0	0.376
GO:0016773	Phosphotransferase activity alcohol group as acceptor	309	−0.29	−1.31	0	0.38
GO:0000122	Negative regulation of transcription from RNA polymerase II promoter	72	−0.37	−1.34	0	0.381
GO:0009607	Response to biotic stimulus	95	−0.55	−1.34	0	0.384
GO:0031667	Response to nutrient levels	29	−0.64	−1.32	0	0.385
GO:0006937	Regulation of muscle contraction	17	−0.58	−1.3	0	0.385
GO:0008283	Cell proliferation	470	−0.44	−1.31	0	0.387

Comparison of [control (n = 4) vs control-SE (n = 4)] vs [Astro-D2KO (n = 4) vs Astro-D2KO-SE (n = 4)] animals at a nominal $P < 0.01$.

Abbreviations: ES, enrichment score; NES, normalized enrichment score.

seizure activity (41). Indeed, in the current study, seizure but not pilocarpine administration triggered *Dio2* expression (Fig. 4H). The expression pattern of T3-responsive genes revealed increased T3-TR signaling in the brain. In addition, *Dio2* mRNA increases 15 minutes into the SE (Fig. 4B). It is also noticeable that once SE is stopped with diazepam, the drop in D2 activity was faster than the drop in *Dio2* mRNA (Fig. 4C and 4D), probably because the D2 ubiquitin ligase WSB-1 (42) is an HIF-inducible gene (43) and its induction is likely to accelerate D2 ubiquitination and degradation.

In coordination with the *Dio2* induction, *Dio3* mRNA levels decreased markedly (Fig. 4E), even though sample variability prevented a statistically significant decrease in D3 activity (Fig. 4F). Although expression of *Dio2* and *Dio3* are often coordinated, a reduction in *Dio3* mRNA during hypoxia is unexpected given that *Dio3* was shown to be upregulated in recently deceased individuals suffering from diseases associated with poor tissue perfusion (44), in postinfarction rat myocardium (45), in right ventricular hypertrophy (46), and in hypoxic neuroblastoma cells in culture (16, 17). Unfortunately, an analysis of the gene pathways activated by SE as seen in Tables 1–4 does not help identify the mechanism that is overriding the HIF-1α induction of *Dio3*. Nevertheless, D3 is seen concentrating in the nucleus of the neurons in the SE CNS (Fig. 3M–3V). This is reminiscent of our previous observations that insult to the CNS, such as ischemia, redirects D3 trafficking to the cell nucleus via induction of Hsp40, enhancing its ability to inactivate T3 and reduce T3-TR signaling (16, 17). In the case of SE animals, *Hsp40* is induced by about fourfold in both control and Astro-D2 mice (Supplemental Tables 2 and 3).

The hippocampus of animals undergoing SE has been previously studied by microarray; the most affected gene pathways fall into the categories included in Tables 2 and 3. The consensus among these studies is that a robust response in gene expression is mounted to adapt and minimize damage resulting from SE (47–49). Therefore, it is important that, in the absence of a functional D2 pathway, as in the Astro-D2KO animals, the hippocampi of SE animals exhibited a unique gene expression profile that was quite different from control-SE animals. The control-SE animals activate gene pathways related to response to oxidative stress, followed by other gene sets involved in cell homeostasis (Table 4). In contrast, the Astro-D2KO-SE animals activate gene sets that reflect accelerated phosphorylation and kinase activity (Table 4). In fact, the list of top 20 genes upregulated in Astro-D2KO-SE include those connected with inflammation, apoptosis, and cell death, suggesting that a functional *Dio2* pathway is critical for the CNS adaptive response that follows SE.

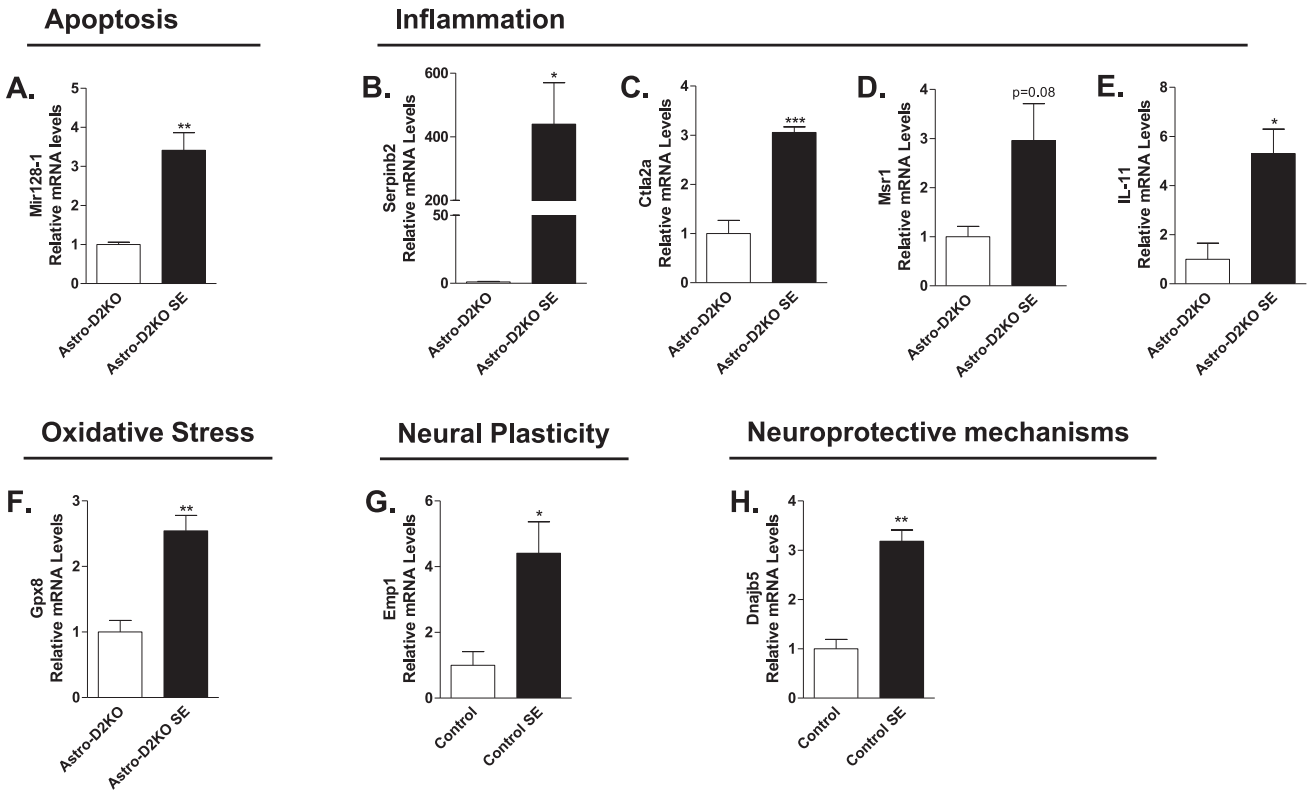

Figure 6. mRNA levels of representative genes identified through analysis of microarray data. All samples are from hippocampi of control-SE or Astro-D2KO-SE mice undergoing 3 hours of SE. In all cases, SE was induced by lithium chloride and pilocarpine administration, as in Fig. 1B. (A) *Mir128-1* mRNA levels in hippocampus of Astro-D2KO mice following pilocarpine-induced SE that were euthanized 3 hours after diazepam injection, measured by RT-qPCR and using *Cyclo A* as internal control (n = 4). (B) *Serpinb2* mRNA levels in hippocampus of Astro-D2KO mice following pilocarpine-induced SE that were euthanized 3 hours after diazepam injection, measured by RT-qPCR and using *Cyclo A* as internal control (n = 4). (C) *Ctla2a* mRNA levels in hippocampus of Astro-D2KO mice following pilocarpine-induced SE that were euthanized 3 hours after diazepam injection, measured by RT-qPCR and using *Cyclo A* as internal control (n = 4). (D) *Msr1* mRNA levels in hippocampus of Astro-D2KO mice following pilocarpine-induced SE euthanized 3 hours after diazepam injection measured by RT-qPCR and using *Cyclo A* as internal control (n = 4). (E) *IL-11* mRNA levels in hippocampus of Astro-D2KO mice following pilocarpine-induced SE that were euthanized 3 hours after diazepam injection, measured by RT-qPCR and using *Cyclo A* as internal control (n = 4). (F) *Gpx8* mRNA levels in hippocampus of Astro-D2KO mice following pilocarpine-induced SE that were euthanized 3 hours after diazepam injection, measured by RT-qPCR and using *Cyclo A* as internal control (n = 4). (G) *Emp1* mRNA levels in hippocampus of control mice following pilocarpine-induced SE that were euthanized 3 hours after diazepam injection, measured by RT-qPCR and using *Cyclo A* as internal control (n = 4). (H) *Dnajb5* mRNA levels in hippocampus of control mice following pilocarpine-induced SE that were euthanized 3 hours after diazepam injection, measured by RT-qPCR and using *Cyclo A* as internal control (n = 4). Values represent the mean ± SEM $*P < 0.05$ vs control with; $**P < 0.01$ vs control with; $***P < 0.001$ vs control.

We conclude that thyroid hormone metabolism and action are affected in the CNS following SE in mice. Not only are traditional T3-responsive genes involved, but so also are a large number of genes that participate in the adaptive response mounted by the CNS following SE. The present studies were performed acutely, only a few hours after SE was terminated. Given that these animals could eventually develop permanent brain damage and spontaneous seizures (50), future studies should clarify whether the Astro-D2KO animals are more or less susceptible to developing a chronic epileptic state.

Acknowledgments

Financial Support: This work was supported by National Institute of Diabetes and Digestive and Kidney Diseases Grant R01 DK65055 (to A.C.B.) and Fundação de Amparo à Pesquisa do Estado de São Paulo, Brazil, Grant 2015/13235-1 (to M.O.R.) and Grant 2013/09133-3 (to B.P.P.N.).

Correspondence: Antonio C. Bianco, MD, PhD, University of Chicago Medical Center, 5841 South Maryland Avenue, Chicago, Illinois 60637. E-mail: abianco@deiodinase.org; or Miriam O. Ribeiro, PhD, Mackenzie Presbyterian University, 930 Rua da Consolação, 01302-907 São Paulo-SP, Brazil. E-mail: miriamribeiro@mackenzie.br.

Disclosure Summary: The authors have nothing to disclose.

References

1. Brent GA. Mechanisms of thyroid hormone action. *J Clin Invest*. 2012;**122**(9):3035–3043.
2. Gereben B, Zavacki AM, Ribich S, Kim BW, Huang SA, Simonides WS, Zeöld A, Bianco AC. Cellular and molecular basis of deiodinase-regulated thyroid hormone signaling. *Endocr Rev*. 2008;**29**(7):898–938.
3. Mohacsik P, Zeold A, Bianco AC, Gereben B. Thyroid hormone and the neuroglia: both source and target. *J Thyroid Res*. 2011; **2011**:215718.
4. Tu HM, Kim SW, Salvatore D, Bartha T, Legradi G, Larsen PR, Lechan RM. Regional distribution of type 2 thyroxine deiodinase

messenger ribonucleic acid in rat hypothalamus and pituitary and its regulation by thyroid hormone. *Endocrinology*. 1997;**138**(8): 3359–3368.
5. Guadaño-Ferraz A, Obregón MJ, St Germain DL, Bernal J. The type 2 iodothyronine deiodinase is expressed primarily in glial cells in the neonatal rat brain. *Proc Natl Acad Sci USA*. 1997;**94**(19): 10391–10396.
6. Bartha T, Kim SW, Salvatore D, Gereben B, Tu HM, Harney JW, Rudas P, Larsen PR. Characterization of the 5′-flanking and 5′-untranslated regions of the cyclic adenosine 3′,5′-monophosphate-responsive human type 2 iodothyronine deiodinase gene. *Endocrinology*. 2000;**141**(1):229–237.
7. Canettieri G, Celi FS, Baccheschi G, Salvatori L, Andreoli M, Centanni M. Isolation of human type 2 deiodinase gene promoter and characterization of a functional cyclic adenosine monophosphate response element. *Endocrinology*. 2000;**141**(5): 1804–1813.
8. Burmeister LA, Pachucki J, St Germain DL. Thyroid hormones inhibit type 2 iodothyronine deiodinase in the rat cerebral cortex by both pre- and posttranslational mechanisms. *Endocrinology*. 1997; **138**(12):5231–5237.
9. Kim SW, Harney JW, Larsen PR. Studies of the hormonal regulation of type 2 5′-iodothyronine deiodinase messenger ribonucleic acid in pituitary tumor cells using semiquantitative reverse transcription-polymerase chain reaction. *Endocrinology*. 1998; **139**(12):4895–4905.
10. Steinsapir J, Harney J, Larsen PR. Type 2 iodothyronine deiodinase in rat pituitary tumor cells is inactivated in proteasomes. *J Clin Invest*. 1998;**102**(11):1895–1899.
11. Gereben B, Goncalves C, Harney JW, Larsen PR, Bianco AC. Selective proteolysis of human type 2 deiodinase: a novel ubiquitin-proteasomal mediated mechanism for regulation of hormone activation. *Mol Endocrinol*. 2000;**14**(11):1697–1708.
12. Bernal J, Guadaño-Ferraz A, Morte B. Perspectives in the study of thyroid hormone action on brain development and function. *Thyroid*. 2003;**13**(11):1005–1012.
13. St Germain DL, Galton VA, Hernandez A. Minireview: defining the roles of the iodothyronine deiodinases: current concepts and challenges. *Endocrinology*. 2009;**150**(3):1097–1107.
14. Tu HM, Legradi G, Bartha T, Salvatore D, Lechan RM, Larsen PR. Regional expression of the type 3 iodothyronine deiodinase messenger ribonucleic acid in the rat central nervous system and its regulation by thyroid hormone. *Endocrinology*. 1999;**140**(2): 784–790.
15. Peeters R, Fekete C, Goncalves C, Legradi G, Tu HM, Harney JW, Bianco AC, Lechan RM, Larsen PR. Regional physiological adaptation of the central nervous system deiodinases to iodine deficiency. *Am J Physiol Endocrinol Metab*. 2001;**281**(1):E54–E61.
16. Freitas BC, Gereben B, Castillo M, Kalló I, Zeöld A, Egri P, Liposits Z, Zavacki AM, Maciel RM, Jo S, Singru P, Sanchez E, Lechan RM, Bianco AC. Paracrine signaling by glial cell-derived triiodothyronine activates neuronal gene expression in the rodent brain and human cells. *J Clin Invest*. 2010;**120**(6):2206–2217.
17. Jo S, Kalló I, Bardóczi Z, Arrojo e Drigo R, Zeöld A, Liposits Z, Oliva A, Lemmon VP, Bixby JL, Gereben B, Bianco AC. Neuronal hypoxia induces Hsp40-mediated nuclear import of type 3 deiodinase as an adaptive mechanism to reduce cellular metabolism. *J Neurosci*. 2012;**32**(25):8491–8500.
18. Margaill I, Royer J, Lerouet D, Ramaugé M, Le Goascogne C, Li WW, Plotkine M, Pierre M, Courtin F. Induction of type 2 iodothyronine deiodinase in astrocytes after transient focal cerebral ischemia in the rat. *J Cereb Blood Flow Metab*. 2005;**25**(4): 468–476.
19. Lamirand A, Mercier G, Ramaugé M, Pierre M, Courtin F. Hypoxia stabilizes type 2 deiodinase activity in rat astrocytes. *Endocrinology*. 2007;**148**(10):4745–4753.
20. Zou L, Burmeister LA, Styren SD, Kochanek PM, DeKosky ST. Up-regulation of type 2 iodothyronine deiodinase mRNA in reactive astrocytes following traumatic brain injury in the rat. *J Neurochem*. 1998;**71**(2):887–890.
21. Wasterlain CG, Fujikawa DG, Penix L, Sankar R. Pathophysiological mechanisms of brain damage from status epilepticus. *Epilepsia*. 1993; **34**(Suppl 1)S37–S53.
22. McNamara JO. Cellular and molecular basis of epilepsy. *J Neurosci*. 1994;**14**(6):3413–3425.
23. Gastaut H, Gastaut JL, Gonçalves e Silva GE, Fernandez Sanchez GR. Relative frequency of different types of epilepsy: a study employing the classification of the International League Against Epilepsy. *Epilepsia*. 1975;**16**(3):457–461.
24. Walczak TS. Neocortical temporal lobe epilepsy: characterizing the syndrome. *Epilepsia*. 1995;**36**(7):633–635.
25. Sutter R, Dittrich T, Semmlack S, Rüegg S, Marsch S, Kaplan PW. Acute systemic complications of convulsive status epilepticus-a systematic review. *Crit Care Med*. 2018;**46**(1):138–145.
26. Fabene PF, Merigo F, Galiè M, Benati D, Bernardi P, Farace P, Nicolato E, Marzola P, Sbarbati A. Pilocarpine-induced status epilepticus in rats involves ischemic and excitotoxic mechanisms. *PLoS One*. 2007;**2**(10):e1105.
27. Fonseca TL, Correa-Medina M, Campos MP, Wittmann G, Werneck-de-Castro JP, Arrojo e Drigo R, Mora-Garzon M, Ueta CB, Caicedo A, Fekete C, Gereben B, Lechan RM, Bianco AC. Coordination of hypothalamic and pituitary T3 production regulates TSH expression. *J Clin Invest*. 2013;**123**(4):1492–1500.
28. Bianco AC, Anderson G, Forrest D, Galton VA, Gereben B, Kim BW, Kopp PA, Liao XH, Obregon MJ, Peeters RP, Refetoff S, Sharlin DS, Simonides WS, Weiss RE, Williams GR; American Thyroid Association Task Force on Approaches and Strategies to Investigate Thyroid Hormone Economy and Action. American Thyroid Association Guide to investigating thyroid hormone economy and action in rodent and cell models. *Thyroid*. 2014; **24**(1):88–168.
29. Turski WA, Cavalheiro EA, Schwarz M, Czuczwar SJ, Kleinrok Z, Turski L. Limbic seizures produced by pilocarpine in rats: behavioural, electroencephalographic and neuropathological study. *Behav Brain Res*. 1983;**9**(3):315–335.
30. Curia G, Longo D, Biagini G, Jones RS, Avoli M. The pilocarpine model of temporal lobe epilepsy. *J Neurosci Methods*. 2008;**172**(2): 143–157.
31. Lévesque M, Avoli M, Bernard C. Animal models of temporal lobe epilepsy following systemic chemoconvulsant administration. *J Neurosci Methods*. 2016;**260**:45–52.
32. Christoffolete MA, Ribeiro R, Singru P, Fekete C, da Silva WS, Gordon DF, Huang SA, Crescenzi A, Harney JW, Ridgway EC, Larsen PR, Lechan RM, Bianco AC. Atypical expression of type 2 iodothyronine deiodinase in thyrotrophs explains the thyroxine-mediated pituitary thyrotropin feedback mechanism. *Endocrinology*. 2006;**147**(4):1735–1743.
33. Diez D, Grijota-Martinez C, Agretti P, De Marco G, Tonacchera M, Pinchera A, de Escobar GM, Bernal J, Morte B. Thyroid hormone action in the adult brain: gene expression profiling of the effects of single and multiple doses of triiodo-L-thyronine in the rat striatum. *Endocrinology*. 2008;**149**(8):3989–4000.
34. Morte B, Ceballos A, Diez D, Grijota-Martínez C, Dumitrescu AM, Di Cosmo C, Galton VA, Refetoff S, Bernal J. Thyroid hormone-regulated mouse cerebral cortex genes are differentially dependent on the source of the hormone: a study in monocarboxylate transporter-8- and deiodinase-2-deficient mice. *Endocrinology*. 2010;**151**(5):2381–2387.
35. Hernandez A, Morte B, Belinchón MM, Ceballos A, Bernal J. Critical role of types 2 and 3 deiodinases in the negative regulation of gene expression by T_3in the mouse cerebral cortex. *Endocrinology*. 2012;**153**(6):2919–2928.
36. Yu G, Tzouvelekis A, Wang R, Herazo-Maya JD, Ibarra GH, Srivastava A, de Castro JPW, DeIuliis G, Ahangari F, Woolard T, Aurelien N, Arrojo E Drigo R, Gan Y, Graham M, Liu X, Homer RJ, Scanlan TS, Mannam P, Lee PJ, Herzog EL, Bianco AC,

Kaminski N. Thyroid hormone inhibits lung fibrosis in mice by improving epithelial mitochondrial function. *Nat Med*. 2018;**24**(1): 39–49.
37. Moore AN, Waxham MN, Dash PK. Neuronal activity increases the phosphorylation of the transcription factor cAMP response element-binding protein (CREB) in rat hippocampus and cortex. *J Biol Chem*. 1996;**271**(24):14214–14220.
38. Lee B, Dziema H, Lee KH, Choi YS, Obrietan K. CRE-mediated transcription and COX-2 expression in the pilocarpine model of status epilepticus. *Neurobiol Dis*. 2007;**25**(1):80–91.
39. Beaumont TL, Yao B, Shah A, Kapatos G, Loeb JA. Layer-specific CREB target gene induction in human neocortical epilepsy. *J Neurosci*. 2012;**32**(41):14389–14401.
40. Hansen KF, Sakamoto K, Pelz C, Impey S, Obrietan K. Profiling status epilepticus-induced changes in hippocampal RNA expression using high-throughput RNA sequencing. *Sci Rep*. 2014;**4**(1):6930.
41. Ferrendelli JA, Blank AC, Gross RA. Relationships between seizure activity and cyclic nucleotide levels in brain. *Brain Res*. 1980; **200**(1):93–103.
42. Dentice M, Bandyopadhyay A, Gereben B, Callebaut I, Christoffolete MA, Kim BW, Nissim S, Mornon JP, Zavacki AM, Zeöld A, Capelo LP, Curcio-Morelli C, Ribeiro R, Harney JW, Tabin CJ, Bianco AC. The Hedgehog-inducible ubiquitin ligase subunit WSB-1 modulates thyroid hormone activation and PTHrP secretion in the developing growth plate. *Nat Cell Biol*. 2005;**7**(7):698–705.
43. Haque M, Kendal JK, MacIsaac RM, Demetrick DJ. WSB1: from homeostasis to hypoxia. *J Biomed Sci*. 2016;**23**(1):61.
44. Peeters RP, Wouters PJ, Kaptein E, van Toor H, Visser TJ, Van den Berghe G. Reduced activation and increased inactivation of thyroid hormone in tissues of critically ill patients. *J Clin Endocrinol Metab*. 2003;**88**(7):3202–3211.
45. Olivares EL, Marassi MP, Fortunato RS, da Silva AC, Costa-e-Sousa RH, Araújo IG, Mattos EC, Masuda MO, Mulcahey MA, Huang SA, Bianco AC, Carvalho DP. Thyroid function disturbance and type 3 iodothyronine deiodinase induction after myocardial infarction in rats a time course study. *Endocrinology*. 2007; **148**(10):4786–4792.
46. Simonides WS, Mulcahey MA, Redout EM, Muller A, Zuidwijk MJ, Visser TJ, Wassen FW, Crescenzi A, da-Silva WS, Harney J, Engel FB, Obregon MJ, Larsen PR, Bianco AC, Huang SA. Hypoxia-inducible factor induces local thyroid hormone inactivation during hypoxic-ischemic disease in rats. *J Clin Invest*. 2008;**118**(3):975–983.
47. Hatazaki S, Bellver-Estelles C, Jimenez-Mateos EM, Meller R, Bonner C, Murphy N, Matsushima S, Taki W, Prehn JH, Simon RP, Henshall DC. Microarray profile of seizure damage-refractory hippocampal CA3 in a mouse model of epileptic preconditioning. *Neuroscience*. 2007;**150**(2):467–477.
48. Hunsberger JG, Bennett AH, Selvanayagam E, Duman RS, Newton SS. Gene profiling the response to kainic acid induced seizures. *Brain Res Mol Brain Res*. 2005;**141**(1):95–112.
49. Lukasiuk K, Pitkänen A. Large-scale analysis of gene expression in epilepsy research: is synthesis already possible? *Neurochem Res*. 2004;**29**(6):1169–1178.
50. Cavalheiro EA, Leite JP, Bortolotto ZA, Turski WA, Ikonomidou C, Turski L. Long-term effects of pilocarpine in rats: structural damage of the brain triggers kindling and spontaneous recurrent seizures. *Epilepsia*. 1991;**32**(6):778–782.